Single-Cell Transcriptomics Reveals Discrete Steps in Regulatory T Cell Development in the Human Thymus

Morgana, Florencia; Opstelten, Rianne; Slot, Manon C.; Scott, Andrew M.; van Lier, René A.W.; Blom, Bianca; Mahfouz, Ahmed; Amsen, Derk

DOI
10.4049/jimmunol.2100506

Publication date
2022

Document Version
Final published version

Published in
Journal of immunology (Baltimore, Md. : 1950)

Citation (APA)
Morgana, F., Opstelten, R., Slot, M. C., Scott, A. M., van Lier, R. A. W., Blom, B., Mahfouz, A., & Amsen, D. (2022). Single-Cell Transcriptomics Reveals Discrete Steps in Regulatory T Cell Development in the Human Thymus. *Journal of immunology (Baltimore, Md. : 1950)*, *208*(2), 384-395. https://doi.org/10.4049/jimmunol.2100506

The Journal of Immunology

RESEARCH ARTICLE | JANUARY 15 2022

Single-Cell Transcriptomics Reveals Discrete Steps in Regulatory T Cell Development in the Human Thymus FREE

Florencia Morgana; ... et. al

J Immunol (2022) 208 (2): 384–395.
https://doi.org/10.4049/jimmunol.2100506

Single-Cell Transcriptomics Reveals Discrete Steps in Regulatory T Cell Development in the Human Thymus

Florencia Morgana,*,† Rianne Opstelten,*,† Manon C. Slot,*,† Andrew M. Scott,‡,§ René A. W. van Lier,*,†,1 Bianca Blom,¶ Ahmed Mahfouz,‖,# and Derk Amsen*,†,**

$CD4^+CD25^+FOXP3^+$ regulatory T (Treg) cells control immunological tolerance. Treg cells are generated in the thymus (tTreg) or in the periphery. Their superior lineage fidelity makes tTregs the preferred cell type for adoptive cell therapy (ACT). How human tTreg cells develop is incompletely understood. By combining single-cell transcriptomics and flow cytometry, we in this study delineated three major Treg developmental stages in the human thymus. At the first stage, which we propose to name pre-Treg I, cells still express lineage-inappropriate genes and exhibit signs of TCR signaling, presumably reflecting recognition of self-antigen. The subsequent pre-Treg II stage is marked by the sharp appearance of transcription factor FOXO1 and features induction of KLF2 and CCR7, in apparent preparation for thymic exit. The pre-Treg II stage can further be refined based on the sequential acquisition of surface markers CD31 and GPA33. The expression of CD45RA, finally, completes the phenotype also found on mature recent thymic emigrant Treg cells. Remarkably, the thymus contains a substantial fraction of recirculating mature effector Treg cells, distinguishable by expression of inflammatory chemokine receptors and absence of CCR7. The developmental origin of these cells is unclear and warrants caution when using thymic tissue as a source of stable cells for ACT. We show that cells in the major developmental stages can be distinguished using the surface markers CD1a, CD27, CCR7, and CD39, allowing for their viable isolation. These insights help identify fully mature tTreg cells for ACT and can serve as a basis for further mechanistic studies into tTreg development. ***The Journal of Immunology*, 2022, 208: 384–395.**

$CD4^+$ regulatory T (Treg) cells that express the transcription factor FOXP3 are critical guardians of immunological tolerance by virtue of their ability to suppress both innate and adaptive immunity (1). Clinical trials using adoptive cell therapy (ACT) with Treg cells are ongoing for the treatment of inflammatory disease and to protect transplanted solid organs from immune-mediated rejection (2). The goal of Treg ACT is to restore the imbalance between Treg and conventional T (Tconv) cells. For this purpose, Treg cells are isolated from patients or donors and expanded in vitro before (re)infusion. A challenge for Treg cell therapy is the retrieval and expansion of stable Treg cells with adequate functional potency (3). Resolving this issue requires a thorough understanding of the heterogeneity within the Treg cell compartment (4–7). One layer of heterogeneity is associated with the ontogeny of these cells. The majority of Treg cells is believed to derive from the thymus (thymic Treg [tTreg] cells), whereas a fraction develops from Tconv cells in the periphery (peripheral Treg [pTreg] cells) (8, 9). Mouse studies have demonstrated that tTreg cells are tightly committed to the Treg cell lineage, whereas pTreg cells can reconvert into Tconv cells upon exposure to inflammatory signals (10–12). Hence, tTreg cells are considered the safest option for Treg ACT. As good markers to distinguish tTreg cells from pTreg cells in blood have not yet been identified in humans (13–15), postnatal thymic tissue has been proposed as an alternative source for safe Treg cells to use in ACT (16). Current insight into tTreg cell differentiation mostly stems from animal models, whereas human tTreg cell development remains poorly defined. Treg cell differentiation is thought to occur at the immature CD4 single-positive stage, although human Treg cell development can also initiate at the $CD4^+CD8^+$ double-positive (DP) stage (17–20). In mice, initiation of the Treg cell developmental program reportedly involves medium to high affinity ligation of an autoreactive TCR on a developing thymocyte to a self-antigen presented by thymic APCs (also known as agonist selection). In the major developmental pathway, this activation results in the induction of CD25, the limiting component of the high affinity IL-2 receptor. Signaling via CD25 subsequently ignites the Treg cell differentiation program, including induction of FOXP3 (17). The Treg cell

*Department of Hematopoiesis, Sanquin Research, Amsterdam, the Netherlands; †Landsteiner Laboratory, Amsterdam UMC, University of Amsterdam, the Netherlands; ‡Tumor Targeting Laboratory, Olivia Newton-John Cancer Research Institute, Melbourne, Australia; §School of Cancer Medicine, La Trobe University, Melbourne, Australia; ¶Department of Experimental Immunology, Amsterdam UMC, University of Amsterdam, Amsterdam, the Netherlands; ‖Department of Human Genetics, Leiden University Medical Center, Leiden, the Netherlands; #Delft Bioinformatics Lab, Delft University of Technology, Delft, the Netherlands; and **Amsterdam Institute for Infection and Immunity, University of Amsterdam, Amsterdam, the Netherlands

[1]Current address: Division of Laboratory, Pharmacy, and Biomedical Genetics, University Medical Center Utrecht, Utrecht, the Netherlands.

ORCID: 0000-0001-8601-2149 (A.M.).

Received for publication May 28, 2021. Accepted for publication November 5, 2021.

This work was supported by Landsteiner Foundation for Blood Transfusion Research Grants 1826 (to R.A.W.v.L.) and 1430 (to D.A.).

F.M., R.O., M.C.S. and D.A. designed the study; F.M. performed the experiments, data analyses, and wrote the manuscript; R.O. contributed to experiments, data interpretation, and manuscript review; M.C.S. performed the cell culture experiments and contributed to data analyses and discussion; A.M.S. provided the GPA33 Ab; R.A.W. and B.B. provided conceptual advice and contributed to the manuscript; A.M. contributed to/supervised the bioinformatic data analyses and interpretation, and contributed to the manuscript; D.A. directed the work, helped with data analyses/interpretation and wrote the manuscript.

The sequence data presented in this study are available from ArrayExpress at the European Bioinformatics Institute (http://www.ebi.ac.uk/arrayexpress) under accession number E-MTAB-11019.

Address correspondence and reprint requests to Dr. Derk Amsen, Department of Hematopoiesis, Sanquin Research and Landsteiner Laboratory, Amsterdam UMC, University of Amsterdam, Plesmanlaan 125, 1066 CX Amsterdam, Noord Holland, the Netherlands. E-mail address: d.amsen@sanquin.nl

The online version of this article contains supplemental material.

Abbreviations used in this article: ACT, adoptive cell therapy; DP, double-positive; pTreg, peripheral Treg; scRNAseq, single-cell RNA sequencing; SORT-seq, sorting and robot-assisted transcriptome sequencing; Tconv, conventional T; Treg, regulatory T; *t*SNE, *t*-distributed stochastic neighbor embedding; tTreg, thymic Treg.

differentiation process is boosted by ligation of costimulatory receptors, such as CD28, GITR, OX40, and CD27, which are induced in response to TCR signaling (21–23). Engagement of these receptors is thought to enhance the expression of CD25, after which auto/paracrine IL-2 activates IL-2 receptor–mediated induction of the Treg cell program (17, 24, 25).

In this study, we examined the composition and development of the human tTreg cell compartment through a combination of single-cell RNA sequencing (scRNAseq) and flow cytometry. We find that a substantial fraction of Treg cells in the human thymus consists of recirculating mature effector Treg cells. These cells exhibit an activated phenotype and can be distinguished from developing Treg cells based on their chemokine receptor profile, most notably the absence of CCR7 expression. Furthermore, we outline a developmental program with several discrete successive steps, which we propose to refer to as follows: 1) pre-Treg I, exhibiting expression of TCR-responsive as well as lineage-inappropriate genes, 2) early pre-Treg II, marked by induction of FOXO1 and upregulation of KLF2 and CCR7 and 3) late pre-Treg II, featuring the sequential appearance of CD31 and GPA33, after which acquisition of CD45RA marks the final step of differentiation into fully mature Treg cells that are ready for thymic egress.

Materials and Methods

Tissue processing, isolation of thymocytes, and sorting for scRNAseq

tTreg cells were retrieved from anonymized human thymic tissue derived from infant patients up to 3 y of age who had undergone open heart surgery at the Leiden University Medical Center. Informed consent was gathered from patients according to the Declaration of Helsinki and was approved by the Medical Ethical Committee of the Leiden University Medical Center. The thymic tissue was finely dissociated with scissors at room temperature, placed in gentleMACS C tubes (Miltenyi Biotech), filled up to 10 ml with MACS buffer (PBS containing 0.5% FCS) and mechanically disrupted with the gentleMACS Dissociator (Miltenyi Biotech). A single-cell suspension was generated by pressing the tissue through a 100-μm cell strainer. Cells were collected in 50-ml Falcon tubes, pelleted through centrifugation (350 × *g* for 10 min at room temperature) using MACS buffer and counted. Thymocytes used for later analysis by FACS were subsequently cryopreserved by resuspending the cells in FCS containing 10% DMSO. Cells were stored in liquid nitrogen for later use.

For the sorting and robot-assisted transcriptome sequencing (SORT-seq), a thymus derived from a 7-wk-old infant was collected from the operation room immediately after surgery, processed using the method described above (without freezing) and prepared for sorting by FACS, all with minimal delay. Cells were incubated for 15 min at room temperature with the following Abs: anti-CD4 PE (SK3), anti-CD8 PerCP-Cy5.5 (SK1), anti-CD25 BV605 (2A3), and anti-CD127 BV421 (A019D5). Near-IR (Life Technologies) was used as a live/dead marker. Live, $CD4^+CD8^+CD25^+$ single cells were sorted in a 384-well prepared plate containing primers and mineral oil using an FACS Aria III (BD Biosciences). Sorting was based on the following gating strategy: from the live (Near-IR-negative) single-cell fraction, all CD4-positive cells were selected in the CD4/CD8 plot and subsequently sorted based on $CD25^+$ expression, thereby including essentially all CD127-expressing cells. After sorting, cells were immediately snap-frozen on dry ice and stored at −80°C prior to shipment (on dry ice) to Single Cell Discoveries. There, single-cell mRNA sequencing was performed according to the SORT-seq protocol (26).

Flow cytometry

Thymocytes were gently thawed using IMDM containing 20% FCS in the presence of DNAse I (Roche Diagnostics). Cells were labeled with the following Abs: anti-CCR7 (G043H7), anti-CXCR3 (G025H7), anti-CXCR6 (K041E5), anti-CCR5 (J418F1), anti-CD3 (UCHT1), anti-CD4 (SK3), anti-CD4 (L200), anti-CD8 (SK1), anti-CD25 (2A3), anti-CD127 (HIL-7R-M21), anti-CD45RA (HI100), anti-CD39 (eBioA1), anti-CD1a (HI149), anti-CD27 (O323), anti-GPA33 (no. 402104), anti-CD31 (WM59), anti-FOXO1 (C29H4), anti-FOXP3 (236A/E7), and anti-TIGIT (A15153G). Surface staining for chemokine receptors was done in PBS containing 0.5% FCS for 15 min at 37°C. Other surface stainings were done in PBS containing 0.5% FCS for 15 min at room temperature. Dead cells were excluded from the analysis using Live/Dead Fixable Yellow (Life Technologies). For intracellular staining of FOXO1 and FOXP3, cells were fixed and permeabilized using the FOXP3/Transcription Factor Fixation/Permeabilization buffers (eBioscience) according to manufacturer's instructions. Data were acquired on an FACSymphony A5 (BD Biosciences) using the FACSDiva software and analyzed using the FlowJo software (version 10.7.1). Statistical tests were performed using Graphpad Prism software (version 8.0.2). Results were considered significant at $p < 0.05$.

Cell culture

Naive Tconv ($CD4^+CD25^-CD127^+CD45RA^+$, control cells isolated from PBMCs), $GPA33^+$ ($CD4^+CD25^+CD39^-GPA33^+$), and $GPA33^-$ ($CD4^+CD25^+CD39^-GPA33^-$) thymocytes were sorted using an FACS Aria III (BD Biosciences). Cells were cultured at 20,000 cells per well in 96-well U-bottom plates (Greiner Bio-One North America) in IMDM + 10% FCS + 1% L-glutamine + 1% penicillin/streptomycin for 7 d in the presence of 0.1 μg/ml soluble anti-CD3 mAb (M1654, clone 1XE; PeliCluster), 0.1 μg/ml anti-CD28 mAb (clone CD8.2; eBioscience) and 300 IU/ml IL-2 (proleukin; Novartis). Cells were harvested and analyzed at day 7.

scRNAseq data analysis

scRNAseq data were loaded into R as a counts matrix and data analysis was performed using the Seurat R package (version 3.0) (27). Quality control was performed by excluding cells expressing fewer than 350 genes (potential empty wells or disintegrated cells) and more than 4000 detected genes (possible doublets). Cells with more than ∼20% of mitochondrial read content were removed as these may correspond to damaged or dying cells (28). Genes not detected in a minimum of three cells (low-abundance genes) were excluded from downstream analysis. Raw counts for gene i in cell j (X_{ij}) were normalized using the Seurat function "NormalizeData" such that $y_{ij} = \ln\left(\frac{X_{ij}}{\sum_i X_{ij}} \times 10^4 + 1\right)$. Highly variable genes were selected using the "FindVariableFeatures" function using the versus method. The data were scaled and centered using the function "ScaleData" and principal component analysis was applied using the highly variable genes. A scree plot was used to determine the number of relevant dimensions, and 12 dimensions were retained for clustering and visualization. A shared nearest-neighbor graph was constructed using "FindNeighbors" and used to identify clusters using the "FindClusters" function with the resolution parameter set to 0.5. Clusters were visualized using *t*-distributed stochastic neighbor embedding (*t*SNE) based on the selected principal components. Marker genes for each cluster were identified using the Wilcoxon rank-sum test in the "FindMarkers" function with default settings and p values adjusted for multiple testing based on Bonferroni. Differentially expressed genes were defined as those with a $\log_2$(fold change) > 0.25 and adjusted p value <0.05. Trajectory analysis was performed using Slingshot (29). The lineage structure is identified with a cluster-based minimum spanning tree using the "getLineages" function, followed by construction of smooth representations of each lineage using simultaneous principal curves using the function "getCurves." For this, a starting cluster was annotated (Cluster 1).

Results

Clustering analysis on $CD4^+CD25^+$ human thymocytes reveals three subpopulations

To study tTreg cell development and differentiation, we performed scRNAseq using an SORT-seq approach. Although FOXP3 is the major Treg cell marker, its detection requires cell permeabilization, which compromises mRNA quality. Viable cells from the tTreg cell lineage were therefore isolated by sorting $CD4^+CD25^+$ cells, most of which are $FOXP3^+$ (Supplemental Fig. 1A; note that this gate includes $CD4^+CD8^+$ DP thymocytes and CD127-expressing cells to avoid selecting against cells in the earliest stages of Treg cell development (30)). This gating strategy captures most thymic $CD4^+FOXP3^+$ cells (Supplemental Fig. 1B), although it excludes small populations of $FOXP3^+CD25^-$ precursors, which have been reported in mice (31), as well as $FOXP3^+CD4^-CD8^-$ double-negative cells, which have also been found in human thymus (32). We sorted 376 Treg cells derived from a human postnatal thymus of a 7-wk-old infant. After quality control of the scRNAseq data, including removal of potential empty wells and doublets, we obtained 344

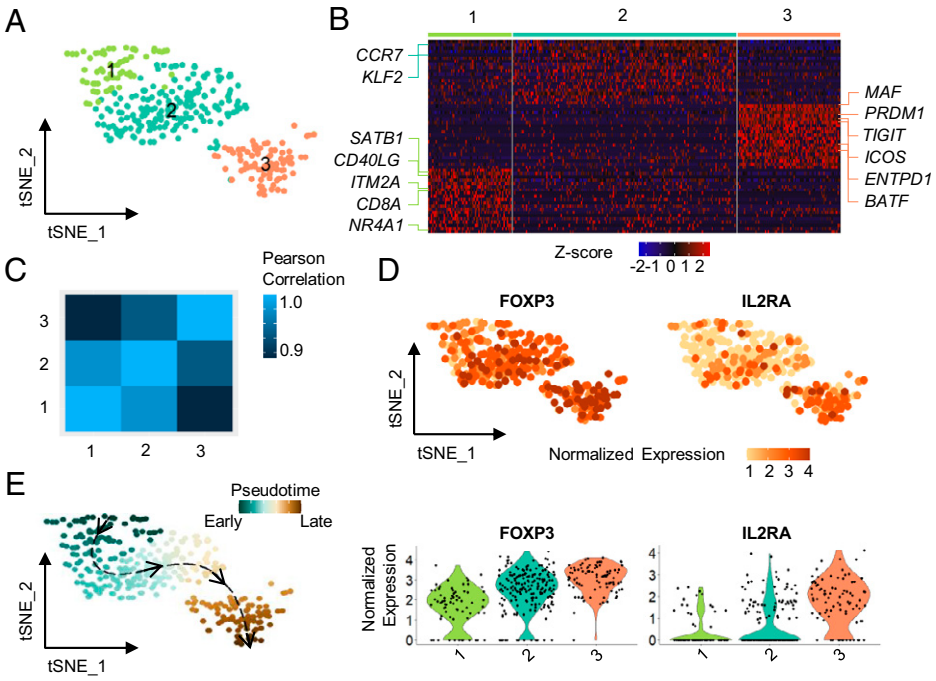

FIGURE 1. Clustering analysis on total $CD4^+CD25^+CD127^{low}$ human thymocytes reveals three clusters. (**A**) scRNAseq was performed on sorted, live $CD4^+CD25^+$ thymocytes. tSNE visualization of graph-based clustering colored by cluster. (**B**) Single-cell feature expression heatmap displaying the top 20 genes per cluster. Selected genes are listed on the side. (**C**) Tile plot visualizing a pairwise correlation of the average expression of Cluster 1, 2, and 3. (**D**) Feature plots (top row) and corresponding violin plots (bottom row) showing the single-cell expression of *FOXP3* and *IL2RA* across the three clusters. (**E**) Trajectory inference analysis performed on the three clusters using Slingshot, with Cluster 1 selected as the root node.

cells. Clustering analysis yielded three populations of cells, which we named Cluster 1, 2, and 3. Of these, Cluster 1 and 2 appeared more closely related to each other, whereas Cluster 3 seemed more distinct (Fig. 1A–C).

We verified the reproducibility of our findings by reanalysing scRNAseq data from a recently published study, in which the total thymocyte population had been examined from multiple donors at different ages (33). We specifically focused on the $IL2RA^+$ fraction of Treg cells from the infant portion of the dataset (comprising three donors), as our data stem from infant-derived $CD25^+$ thymocytes. Clustering analysis yielded two major clusters, which encompassed three Treg cell populations, corresponding to the Treg cell populations identified in that study (33) (Supplemental Fig. 2A). Indeed, expression patterns of key genes from our own dataset (elaborated upon further down), were very similar in this independent dataset (Supplemental Fig. 2D–H), bolstering confidence in the general validity of our results.

A clear expression gradient of the hallmark Treg cell factors *FOXP3* and *IL2RA* (CD25) could be observed in our data, ranging from relatively low in Cluster 1 to high in Cluster 3 (Fig. 1D). This pattern might suggest that these clusters represent subsequent stages of development. Support for this idea came from a bioinformatic trajectory inference analysis using Slingshot, which predicts developmental trajectories based on the degree of similarity between clusters in the composition of the full transcriptomes (29). Making the assumption that low expression of *FOXP3* and *IL2RA* marks the earliest stage of Treg cell development, this analysis suggested that the developmental trajectory would proceed from Cluster 1 via Cluster 2 to Cluster 3 (Fig. 1E). Similar results were obtained when examining the $IL2RA^+$ infant-derived cells from the data set published by Park et al. (33) (Supplemental Fig. 2B, 2C).

The human postnatal thymus contains a population of recirculating effector Treg cells

Cells in Cluster 3 exhibited a highly activated phenotype, strongly expressing genes associated with effector function and activation, including *ENTPD1* (CD39), *MAF*, *ICOS*, *TIGIT*, *TNFRSF18* (GITR), *PRDM1* (Blimp-1), *CTLA4,* and *BATF* (Fig. 2A–C). The idea that these cells would be at the final stage of tTreg cell differentiation seems at odds with the resting phenotype of recent thymic emigrant Treg cells found in the periphery (34). Hence, we considered two alternative possibilities. One option was that these cells, contrary to the predictions of the trajectory inference analysis, in fact reside at a relatively early stage of tTreg cell development and have just undergone agonist selection. The TCR stimulation they receive during this stage in development would then explain their activated phenotype. Alternatively, cells in this cluster may actually not represent a stage during thymic development but might instead be mature effector Treg (eTreg) cells that have recirculated from the periphery into the thymus. Indeed, unlike cells in Cluster 1 and 2, these cells highly expressed genes encoding chemokine receptors involved in migration toward inflamed tissue, including *CXCR3*, *CXCR6*, and *CCR5* (35, 36) (Fig. 2D). Conversely, *CCR7*, a chemokine receptor required for thymocyte migration from the cortex to the thymic medulla and associated with migration toward secondary lymphoid organs (37), was clearly expressed on cells in Clusters 1 and 2, but conspicuously absent from cells in Cluster 3 (Fig. 2D). The same mRNA expression patterns could also be observed upon reanalysis of the dataset from Park et al., underscoring the robustness of these findings (38) (Supplemental Fig. 2D, 2E). Moreover, we validated these findings at the protein level using flow cytometry, which showed clear coexpression between CD39 (encoded by *ENTPD1*), one of the effector molecules highly expressed by cells in Cluster 3, and the inflammatory chemokine receptors CXCR3, CXCR6, and CCR5. Protein expression of CD39 and CCR7 was, however, mutually exclusive (Fig. 2E, 2F). Together, these results indicate that cells in Cluster 3 of the tSNE analysis represent mature eTreg cells, which possibly recirculated to the thymus from the periphery, as has been described (39, 40). This interpretation is further supported by the observation that the cells in Cluster 3 prominently express BST2 mRNA (Fig. 2A, Supplemental Fig. 3A, 3B), which, together with CCR5, was found to identify fully functional Treg cells (41).

Cluster 1 represents the most immature phase in tTreg cell development

Considering that cells in Cluster 3 likely represent a recirculating population of eTreg cells, we focused on the remaining two clusters

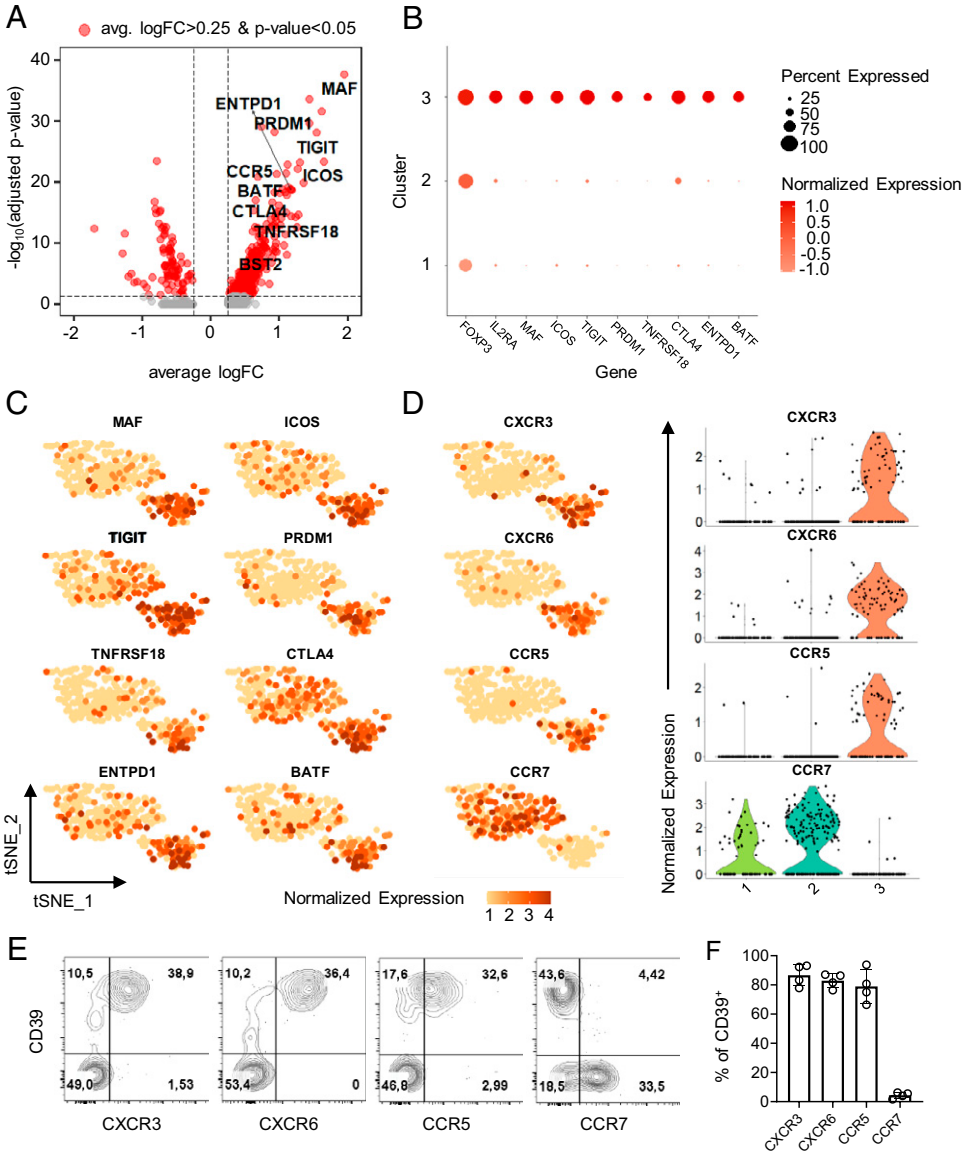

FIGURE 2. The human postnatal thymus contains a population of recirculating effector Treg cells. (**A**) Volcano plot comparing the single-cell gene expression profiles of Cluster 3 versus the rest (Cluster 1 and 2). (**B**) Dot plot showing the transcriptomic expression of selected key genes of Cluster 3 across all clusters. (**C**) Feature plots showing the transcriptomic single-cell expression pattern of *MAF*, *ICOS*, *TIGIT, PRDM1*, *TNFRSF18*, *CTLA4*, *ENTPD1,* and *BATF*. (**D**) Feature plots (left column) and violin plots (right column) displaying the transcriptomic expression pattern and distribution of genes encoding chemokine receptors *CXCR3*, *CXCR6, CCR5,* and *CCR7* across all three clusters. (**E**) Representative flow cytometry contour plots of total $CD4^+CD25^+$ thymocytes showing the protein expression of chemokine receptors CXCR3, CXCR6, CCR5, and CCR7 against CD39 ($n = 4$). (**F**) The frequency of $CXCR3^+$, $CXCR6^+$, $CCR5^+$, and $CCR7^+$ cells within the $CD25^+CD39^+$ gate was quantified ($n = 4$). (E and F) Gating strategy is shown in Supplemental Fig. 1A. Data are representative from two independent experiments with each two patients. Symbols represent individual samples. Shown is the mean ± SD.

(Cluster 1 and 2) to map the tTreg cell developmental program. We found that cells in Cluster 1 expressed *CD40LG* and *CD8A,* whereas expression of these genes was almost absent in Clusters 2 and 3 (Fig. 3A, 3B). Expression of *CD8A* mRNA indicates that these cells have not yet or only recently turned off the CD8 gene, consistent with earlier findings that induction of Treg cell development in the human thymus can already occur at the $CD4^+CD8^+$ DP stage (17, 18). Likewise, *CD40LG* is characteristically not expressed by mature Treg cells. Its expression in this cluster, but not in the others, is therefore also consistent with an early immature stage of Treg cell development. In addition, expression of *NR4A1* was enriched in Cluster 1 (Fig. 3C). *NR4A1* reportedly influences the efficiency of selection as well as the size of the tTreg cell population (42, 43). Importantly, this immediate early gene responds to TCR signaling and is often used as a reporter for this process (44). The expression of *NR4A1* is therefore in line with the idea that cells in Cluster 1 are undergoing agonist selection. That Cluster 1 represents the least mature stage of Treg cell development is supported, finally, by the expression of *ITM2A* and the chromatin organizer *SATB1*, which was highest in Cluster 1 and gradually decreased in Cluster 2 and 3 (Fig. 3C). In mice, *ITM2A* expression is induced in thymocytes during positive selection, but is lost in mature T cells (45), whereas the expression of *SATB1* is high in DP thymocytes, and gradually downregulated during Treg cell development (45, 46).

Identifying a discrete maturation step in Cluster 2

Our findings suggested that a more mature stage of tTreg cell development is represented by cells in Cluster 2. Remarkable in this cluster was the appearance of *KLF2* expression (Fig. 3D). This transcription factor is upregulated upon maturation of conventional thymocytes and controls expression of the S1P1 receptor, which promotes egress from the thymus (47–48). KLF2 also controls the expression of CCR7, necessary for the localization in T cell areas in secondary lymphoid tissue (47). Correspondingly, expression of this chemokine receptor was highest in Cluster 2 (Fig. 2D). These results suggest that cells in Cluster 2 are likely in the latest stages of Treg cell development, preparing to migrate from the thymus to secondary lymphoid organs. Intriguingly, we observed a sharp induction of *FOXO1* expression in Cluster 2 compared with the immature population of cells in Cluster 1 (Fig. 3D). Murine studies have demonstrated the importance of the transcription factor FOXO1 in tTreg cell differentiation as well as in Treg cell function (49). An important function of FOXO1 is to transactivate the *FOXP3* promoter

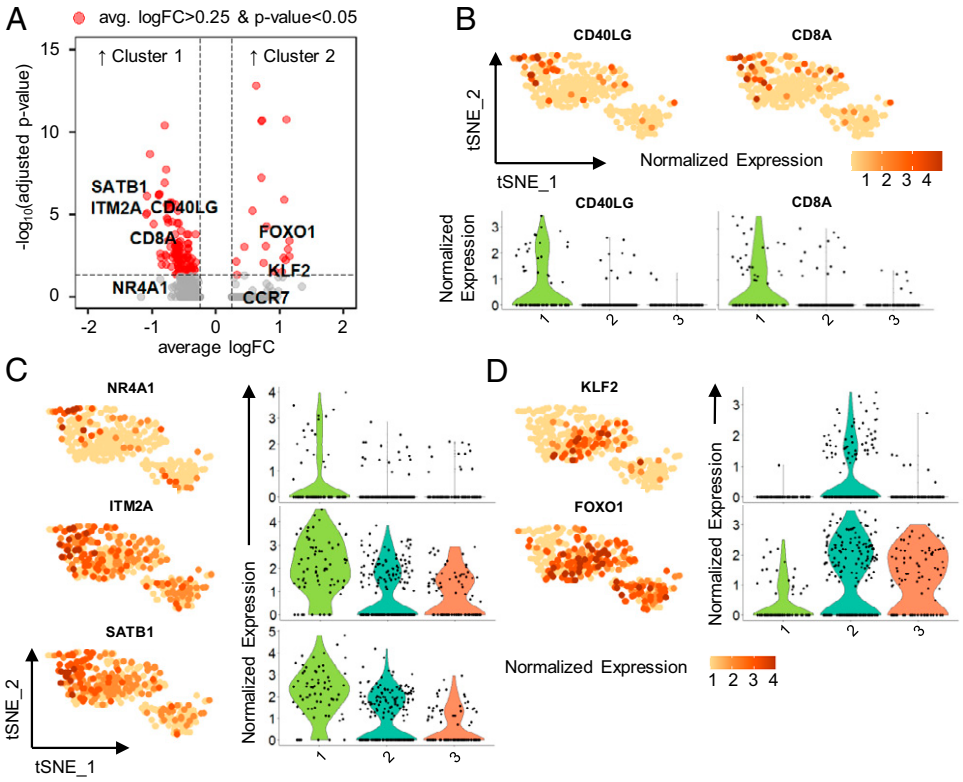

FIGURE 3. Cluster 1 and 2 represent subsequent stages in tTreg cell development. (**A**) Volcano plot showing differentially expressed genes of Cluster 1 (left) versus Cluster 2 (right). (**B**) Feature plots (top) and violin plots (bottom) showing the transcriptomic expression pattern of *CD40LG* and *CD8A*. (**C**) Feature plots (left column) and violin plots (right column) showing the transcriptomic expression pattern of *NR4A1*, *ITM2A,* and *SATB1*. (**D**) Feature plots (left) and violin plots (right) showing the transcriptomic expression pattern of *KLF2* and *FOXO1*.

(50). Indeed, cells in Cluster 2 exhibited higher expression of FOXP3 mRNA than those in Cluster 1 (Fig. 1D).

Given their discrete differences in expression among the clusters found in the transcriptome analysis, we examined whether FOXO1, CD39, and CCR7 can be used to identify the corresponding cell populations by flow cytometry. For this, we specifically examined $CD4^+CD25^+$ infant-derived thymocytes, applying a similar gating approach as used for the scRNAseq sort (Supplemental Fig. 1A). Using a tSNE visualization (51) on $CD4^+CD25^+$ thymocytes derived from three concatenated donors, we detected three cell populations based on FOXO1, CD39, and CCR7 expression (Fig. 4A) (1): $FOXO1^-CD39^-CCR7^{low}$ (solid line) (2), $FOXO1^+CD39^-CCR7^+$ (dashed line), and (3) $FOXO1^+CD39^{high}CCR7^{low}$ (dash-dot line). Based on their expression patterns, these populations resembled Clusters 1, 2, and 3 from the scRNAseq analysis, suggesting that these three markers can be used to identify the corresponding populations by flow cytometry.

Upon closer inspection of the protein expression patterns of FOXO1 and CCR7 using a traditional dot plot visualization, we detected four cell populations of which three resembled the expression patterns of the clusters from the scRNAseq (i.e., $FOXO1^-CCR7^-$ [similar to Cluster 1], $FOXO1^+CCR7^+$ [similar to Cluster 2], and $FOXO1^+CCR7^-$ [similar to Cluster 3]) (Fig. 4B). A small fourth population of $FOXO1^-CCR7^{low}$ cells could also be identified. This population was not recognized as such in the scRNAseq analysis. However, some *CCR7* mRNA expression was found in Cluster 1 (Fig. 1C), even though *FOXO1* mRNA is largely absent in that cluster (Fig. 3D). It seems likely that the $FOXO1^-CCR7^-$ and the $FOXO1^-CCR7^{low}$ populations are too similar to permit separation by the single-cell transcriptome clustering algorithms, at least in our experiment.

CD39 mRNA was uniquely expressed in the activated recirculating population of cells in Cluster 3. Correspondingly, the $FOXO1^+CCR7^-$ cell fraction, which resembled our Cluster 3 cells, exhibited nearly uniform high surface expression of CD39 protein, whereas the expression of this molecule was negligible in the $FOXO1^-CCR7^-$ and $FOXO1^+CCR7^+$ populations (Fig. 4C). The expression of FOXP3 and (to a lesser extent) CD25 followed the pattern found in the scRNAseq analysis: expression was lowest in the $FOXO1^-CCR7^-$ population, elevated in the $FOXO1^+CCR7^+$ fraction and highest in the $FOXO1^+CCR7^-$ population of Treg cells, similar to Clusters 1, 2, and 3 from the transcriptome analysis, respectively (Fig. 4D). Expression of FOXP3 protein strongly correlated with expression of FOXO1, consistent with a role for FOXO1 in inducing expression of the *FOXP3* gene (Fig. 4E). Indeed, the percentage of $FOXO1^+FOXP3^-$ cells was significantly higher than the proportion of $FOXO1^-FOXP3^+$ cells, suggesting that FOXO1 expression generally precedes FOXP3 induction (Fig. 4E).

CD1a and CD27 have previously been used to distinguish early and late developing Treg cells (52). Briefly, thymocytes have been subdivided in three developmental stages (1): the most immature $CD1a^+CD27^-$ cells, progressing via a (2) $CD1a^+CD27^+$ stage to (3) the most mature $CD1a^-CD27^+$ stage (52). Consistent with the developmental progression we had deduced from the scRNAseq results, we observed the highest expression of CD1a and the lowest expression of CD27 to be in the $FOXO1^-CCR7^-$ fraction (similar to Cluster 1 and the $FOXO1^-CD39^-CCR7^{low}$ tSNE population), confirming that these cells were at an early stage of tTreg cell development (Fig. 4F). In contrast, $FOXO1^+CCR7^+$ and $FOXO1^+CCR7^-$ cells (which resembled Clusters 2 and 3, respectively) were low in CD1a but had a higher expression of CD27, suggesting that these cells were more mature than the $FOXO1^-CCR7^-$ cells (Fig. 4F). Together, these results demonstrate that the populations detected using flow cytometry exhibit strong overlap with the three clusters from our scRNAseq dataset, supporting the validity of our scRNAseq analysis. Moreover, these analyses identified surface molecules, that allow the isolation of viable cells in each of these developmental stages for further functional investigation. That is, the most immature $CD4^+CD25^+$ Treg lineage ($FOXP3^{-/low}$-$FOXO1^-$) population (Cluster 1) is $CCR7^-CD1a^+CD27^-CD39^-$,

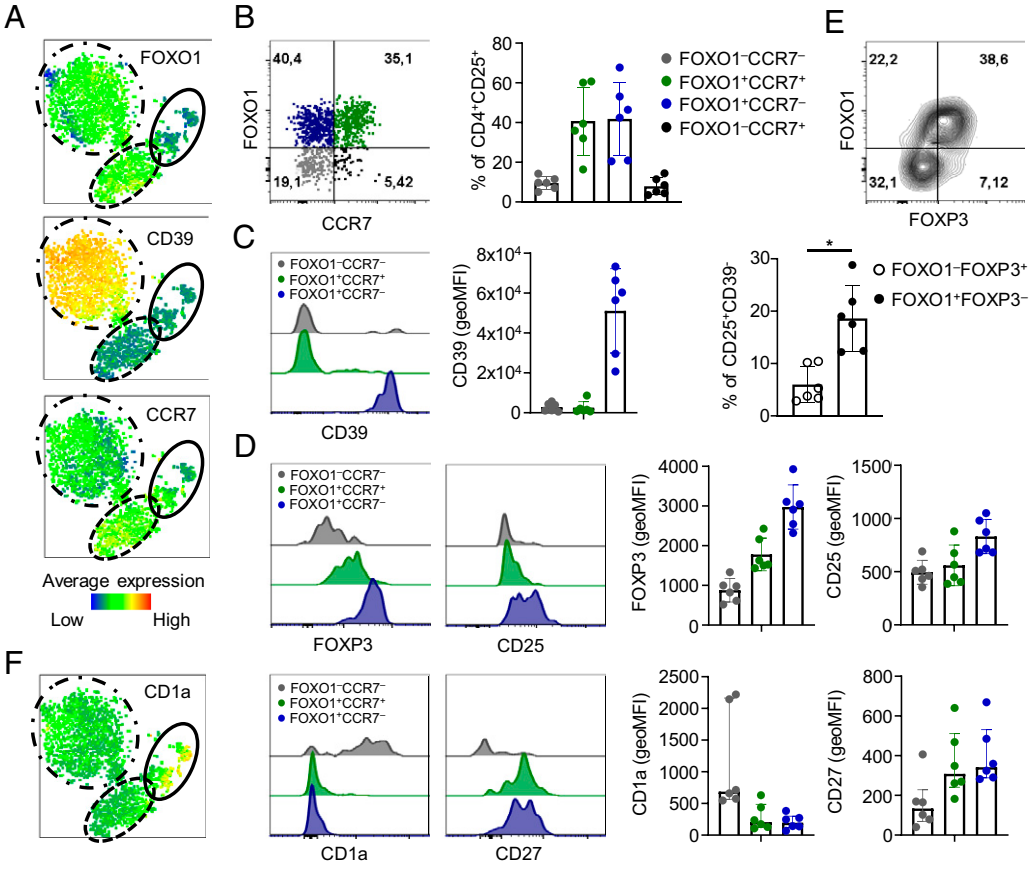

FIGURE 4. FOXO1, CD39, and CCR7 identify the major tTreg subsets. (**A**–**F**) Thymocytes were measured by flow cytometry and gated for $CD4^+CD25^+$ cells for further analysis. (A and F) tSNE maps were generated (based on the markers CD3, CD4, CD8, CCR7, CD25, CD127, CD45RA, CD39, CD1a, CD27, GPA33, CD31, FOXP3, FOXO1, and Helios) in FlowJo (version 10.7.1) using an opt-SNE algorithm[39]. (A) tSNE visualization showing the relative protein expression of FOXO1 (top), CD39 (middle), and CCR7 (bottom) ($n = 3$). (B) Representative flow cytometry dot plot (left) and frequencies (right) showing protein expression of FOXO1 against CCR7, separating the cells in an $FOXO1^-CCR7^-$ (gray), $FOXO1^+CCR7^+$ (green) $FOXO1^+CCR7^-$ (blue), and $FOXO1^-CCR7^+$ (black) population ($n = 6$). (C) Flow cytometry histograms (left) and quantification (right) for CD39 within the indicated populations of $CD4^+CD25^+$ thymocytes ($n = 6$). (D) Representative flow cytometry histograms for FOXP3 (left plot) and CD25 (right plot) within the indicated populations of $CD4^+CD25^+$ thymocytes, identified by the colors as in (B). Average expression levels (geoMFI, right) within the indicated populations ($n = 6$). (E) Representative flow cytometry contour plot (top) and frequencies (bottom) for FOXO1 against FOXP3 on $CD4^+CD25^+CD39^-$ thymocytes. (F) tSNE plot showing intensity of CD1a expression (far left), flow cytometry histograms (second and third plot) and expression levels (geoMFI, fourth and fifth plot; $n = 6$) for CD1a (left) and CD27 (right) within the indicated populations ($n = 6$). (A–F) Gating strategy is shown in Supplemental Fig. 1. Data are representative from two independent experiments with each three patients. Symbols represent individual samples. Shown is the mean ± SD. *$p < 0.05$, paired *t* test. geoMFI, geometric mean fluorescence intensity.

whereas the ($FOXP3^{int}FOXO1^+$) population (Cluster 2) is identifiable by a $CCR7^+CD1a^-CD27^+CD39^-$ phenotype. Recirculating eTreg cells in the thymus finally exhibit a $CCR7^-CD1a^-CD27^+CD39^+$ surface phenotype.

A population of $CD25^-FOXP3^+$ thymocytes exhibits an early immature phenotype

Earlier studies showed the existence of a $CD25^-FOXP3^+$ Treg cell precursor population in mice (31). Although these cells were excluded from the SORT-seq analysis, we could analyze them by flow cytometry for the markers identified above. $CD4^+CD25^-FOXP3^+$ (Supplemental Fig. 4A) displayed minimal expression of CD1a and were only partially positive for CD27, CCR7, FOXO1, and Helios (Supplemental Fig. 4B). This suggests that these cells may be in transit from the most immature stage defined by Cluster 1 to the more mature stage defined by Cluster 2.

GPA33 defines further developmental steps

To determine whether the developmental map of tTreg cells can be further defined, we examined the expression of GPA33. This surface molecule is uniformly found on naive Treg cells in peripheral human blood, suggesting that its expression may be acquired at some point during tTreg cell development (53). *GPA33* was not strongly detected at the transcriptome level in our dataset (Fig. 5A). Nevertheless, a trend toward enrichment for the expression of *GPA33* was present in Cluster 2, the more mature population of developing Treg cells (Fig. 5A). Expression of *GPA33* was absent from cells in Cluster 3, as is the case for most effector Treg cells found in human blood (53), and from Cluster 1 that contains the least mature cells (Fig. 5A). Verification by flow cytometry confirmed that $GPA33^+$ cells in the tTreg lineage lacked expression of CD1a (Fig. 5B), a marker for the most immature cells. Indeed, GPA33 was found exclusively on $FOXO1^+CCR7^+$ tTreg cells (Fig. 5C), which correspond to Cluster 2 from the single-cell transcriptome analysis.

GPA33 is acquired at a late stage of Treg cell development

Based on the expression pattern of CD1a, we hypothesized that $GPA33^-$ tTreg cells are precursors of $GPA33^+$ tTreg cells. Indeed, a substantial fraction of $CD39^-GPA33^-$ tTreg cells (which

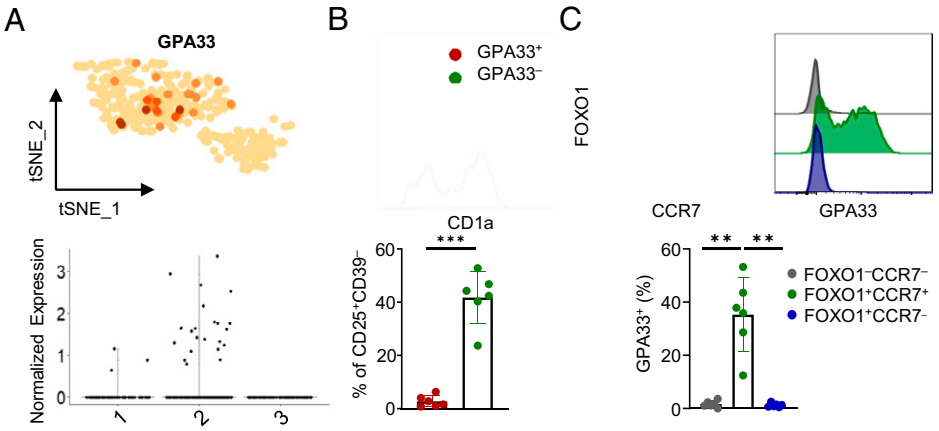

FIGURE 5. GPA33 defines further developmental steps in the pre-Treg II phase. (**A**) Feature plot (top) and violin plot (bottom) showing the transcriptomic single-cell expression pattern and distribution of *GPA33* among tTregs (as in Fig. 1). (**B**) Representative flow cytometry histograms (top) and expression levels (bottom) for CD1a within the indicated populations of $CD4^+CD25^+CD39^-$ thymocytes. (**C**) Representative flow cytometry dot plot for FOXO1 and CCR7 (top, left) and histograms for GPA33 in the three indicated fractions (top, right) within the thymic $CD4^+CD25^+$ population. Percentages of $GPA33^+$ cells within the indicated populations were quantified (bottom). (B and C) Gating strategy is shown in Supplemental Fig. 1. Data are representative from two independent experiments with three patients each. Symbols represent individual samples. Shown is the mean ± SD. $^{**}p < 0.01$, $^{***}p < 0.001$, paired *t* test (B), one-way ANOVA (C).

exclude the $CD39^+$ mature eTreg population) became $GPA33^+$ during in vitro culture with anti-CD3, anti-CD28, and IL-2, whereas $CD39^-GPA33^+$ tTreg cells retained expression of this receptor (Fig. 6A). Furthermore, nearly all tTreg cells that were already $GPA33^+$ before culture, expressed TIGIT after in vitro culture in the presence of anti-CD3, anti-CD28, and IL-2 (Fig. 6B). In sharp contrast, little TIGIT was expressed by those cells that remained $GPA33^-$ during such culture, whereas part of the cells that had acquired GPA33 during culture also expressed TIGIT (Fig. 6B). The extent of TIGIT expression in the $GPA33^+$ tTreg cell population may be associated with the acquisition of specialized functional properties, as previous studies have demonstrated the importance of this molecule in Treg cell function as well as lineage stability (54–56). These results therefore support a model, in which expression of GPA33 marks an advanced stage of Treg cell development in the thymus.

GPA33 expression in the $FOXO1^+CCR7^+$ population was heterogeneous (Fig. 5C), indicating that further developmental steps may be defined by GPA33 among cells in Cluster 2. Indeed, expression of CCR7 was markedly lower among $GPA33^-$ cells in the $FOXO1^+CCR7^+$ population than among $GPA33^+$ cells (Fig. 7A, gating strategy shown in Supplemental Fig. 1C), suggesting that within this population, GPA33 marks the more mature cells.

Reportedly, RTE Treg cells exhibit a $CD31^+CD45RA^+GPA33^+$ phenotype (53, 57). To obtain an indication of when these markers are acquired, we examined their expression pattern among the populations defined by expression of FOXO1 and CCR7. Similar to GPA33 (Fig. 5C), expression of CD31 and CD45RA is found almost exclusively on thymic $FOXO1^+CCR7^+$ Treg lineage cells (Fig. 7B). Within this population, CD45RA expression is mostly found on cells also expressing CD31, with a minor fraction of cells expressing CD45RA, but not CD31, as was reported previously

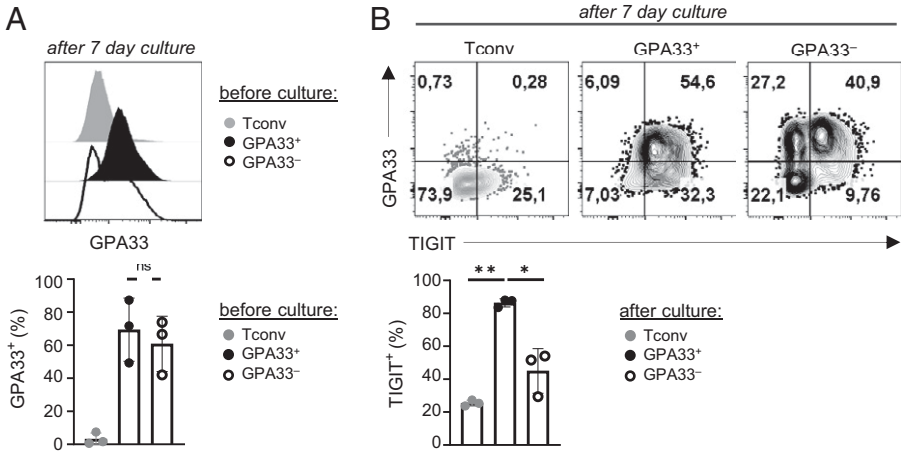

FIGURE 6. GPA33 is acquired at a late stage of Treg cell development. (**A** and **B**) $GPA33^+$ and $GPA33^-$ $CD4^+CD25^{+.}$ thymocytes or $CD4^+CD25^-CD127^+CD45RA^+$ Tconv from peripheral blood were sorted and cultured with anti-CD3, anti-CD28, and IL-2. (A) Representative flow cytometry histograms (top) for GPA33 within the indicated populations after 7 d of in vitro culture. The average frequency (bottom) of GPA33 expression within the indicated populations ($n = 3$). (B) Representative flow cytometry contour plots showing expression of GPA33 against TIGIT in the populations cultured and identified by colors as in (A) (top). The frequencies (bottom) of TIGIT expression within the indicated populations ($n = 3$). Gating strategy is shown in Supplemental Fig. 1. Data are representative from three independent experiments. Symbols represent individual samples. Shown is the mean ± SD. ns, $p > 0.05$, $^*p < 0.05$, $^{**}p < 0.01$, paired *t* test (A), one-way ANOVA (B).

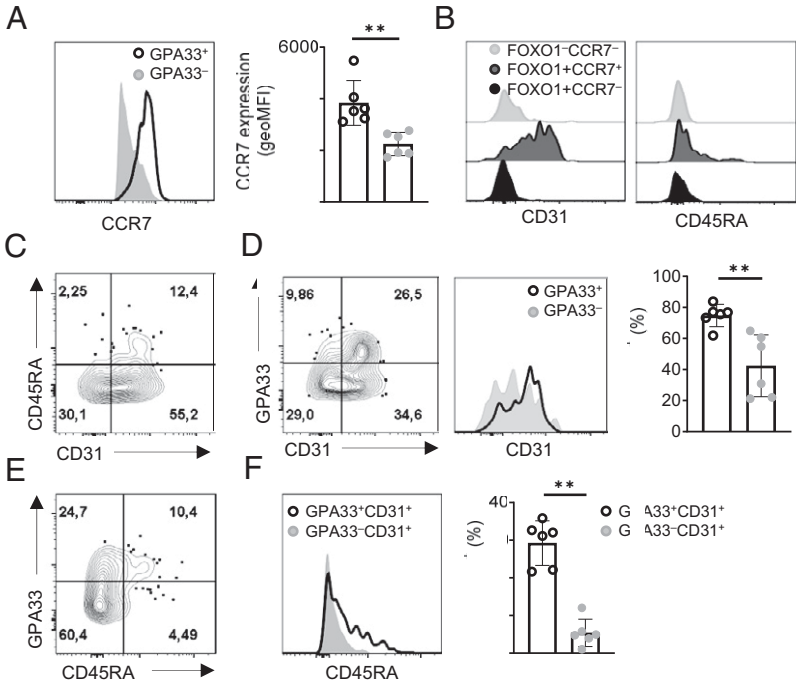

FIGURE 7. CD31, GPA33, and CD45RA are acquired sequentially in the late pre-Treg II stage. (**A** and **C**–**E**) Thymocytes were measured by flow cytometry and gated for $CD4^+CD25^+CD127^{low}FOXO1^+CCR7^+$ cells (Cluster 2) for further analysis. (A) Representative flow cytometry histograms (*left*) and expression levels (geoMFI, right) for CCR7 within the indicated populations ($n = 6$). (**B**) Representative flow cytometry histograms showing the expression of CD31 (*left*) and CD45RA (*right*) within the indicated populations of $CD4^+CD25^+$ thymocytes ($n = 6$). (C) Representative flow cytometry contour plot showing expression of CD45RA against CD31 of $CD4^+CD25^+FOXO1^+CCR7^+$ thymocytes ($n = 6$). (D) Representative flow cytometry contour plot (*left*), histograms (middle) and frequencies (*right*) for GPA33 and CD31 within the $CD4^+CD25^+FOXO1^+CCR7^+$ (Cluster 2) population. (E) Representative flow cytometry contour plot showing expression of GPA33 against CD45RA within the $CD4^+CD25^+FOXO1^+CCR7^+$ (Cluster 2) population. (**F**) Representative flow cytometry histograms (*left*) and frequencies (*right*) for CD45RA within the indicated populations ($n = 6$). (A–E) Gating strategy is shown in Supplemental Fig. 1 with an additional gating on the $CD31^+$ fraction (F). Data are representative from two independent experiments with $n = 3$ patients each. Symbols represent individual samples. Shown is the mean ± SD. $^{**}p < 0.01$, $^{***}p < 0.001$, paired *t* test. geoMFI, geometric mean fluorescence intensity.

(57). In contrast, many $CD31^+$ cells lack expression of CD45RA (Fig. 7C). Likewise, most thymic $FOXO1^+CCR7^+$ Treg lineage cells expressing GPA33 are also positive for CD31, although CD31 single-positive and some $CD31^-GPA33^{-/low}$ cells are also found (Fig. 7D). Because RTE $CD4^+$ T cells generally have a $CD31^+CD45RA^+GPA33^+$ phenotype (53), these results suggest that in the major Treg cell developmental route, tTreg cells acquire expression of CD31 before expression of CD45RA and GPA33. Moreover, all $CD45RA^+$ cells also expressed GPA33 (Fig. 7E), whereas only a fraction of $GPA33^+CD31^+$ cells coexpressed CD45RA (Fig. 7F). The most parsimonious interpretation of these data seems that GPA33 expression is acquired after expression of CD31, but before expression of CD45RA.

Discussion

By combining transcriptomic and protein data, we defined the Treg lineage compartment in the human thymus and provide a model for human tTreg cell development. A prominent Treg cell population (Cluster 3) exhibited a strongly activated phenotype. We considered that this activated phenotype could reflect signaling via the many receptors involved in the induction of the Treg cell program. The population would then represent an intermediate developmental stage between the immature cells in Cluster 1 and the more mature resting cells in Cluster 2. This hypothesis was, however, not supported by a bioinformatic trajectory inference analysis. Moreover, the cells in Cluster 3 conspicuously lacked expression of CCR7. This chemokine receptor controls thymocyte migration from the thymic cortex to the medulla (associated with maturation) and facilitates later homing to peripheral lymphoid tissues by mature naive Treg cells (58–60). CCR7 expression is found in the cells in Cluster 1 and at greater abundance in Cluster 2, which seems consistent with these roles for CCR7 and a gradual acquisition of this receptor. In contrast, a function for transient loss of CCR7 during an intermediate stage is not obvious. The activation-associated genes in Cluster 3 are typically expressed by mature effector Treg cells in the periphery (61, 62). We, therefore, believe that the cells in Cluster 3 represent mature Treg cells that recirculated to the thymus. This phenomenon was documented in mice (63–65) where the Treg cells that migrated from the periphery into the thymus similarly exhibited an activated phenotype and lacked expression of CCR7. Entry into the murine thymus by mature Treg cells was partially dependent on expression of CCR6 (63). This chemokine receptor was not detected in our single-cell transcriptome analysis. However, multiple other chemokine receptors were prominently expressed in these cells, including CXCR3, CCR5, and CXCR6, possibly explaining why deficiency for CCR6 did not abrogate localization of recirculating Treg cells in the murine thymus (63).

The function of a mature, activated Treg cell population in the thymus is not clear. Effector Treg cells may inhibit the development of new Treg cells, possibly to limit the dilution of the repertoire of TCRs in the Treg cell pool with unproven specificities (39). However, evidence also exists that these cells shield Treg cell development from inhibition by inflammatory signals (40). Whichever the function, their presence in the thymus fits with the growing notion that tissues have their own resident population of Treg cells (66), as found for

instance in adipose and muscle tissue and in the lamina propria of the intestinal mucosa (67–69). Development of tissue-resident Treg cells involves initial activation in secondary lymphoid organs and is controlled by the transcription factor BATF (70), which we correspondingly found to be prominently expressed in the cells in Cluster 3.

Evidence for the presence of mature recirculating Treg cells in the human thymus has been provided before (39). In that study, CD31 was proposed as a marker to distinguish between recirculating and developing Treg cells in the thymus. However, our data show that absence of CD31 is not sufficient to reliably identify this population, as also less mature developing Treg cells lack this receptor. Instead, we show that surface expression of CD39 and lack of CCR7 more adequately identify this population within the $CD4^+CD25^+$ fraction of thymocytes.

The residence of recirculating mature Treg cells in the thymus has several implications. First, it means that we cannot ascribe a thymic origin to a Treg population found in the periphery, merely based on the presence of Treg cells with a similar phenotype in the thymus. A thymic origin was, for instance, assigned on this basis to a population of IL-10–producing $ICOS^+$ Treg cells in human blood (38). The nearly uniform expression of ICOS mRNA in Cluster 3 suggests that this is the same population. This notion is further supported by the expression in this Cluster of mRNA encoding the transcription factors BLIMP-1 and MAF, which control the differentiation of IL-10–producing Treg cells (71, 72). As these cells likely recirculated from the periphery to the thymus, it is impossible to know whether they developed into Treg cells in the thymus or in the periphery.

Of clinical importance, the presence of recirculating Treg cells in the thymus stresses the need for caution when using this tissue to obtain Treg cells for ACT (16), because not all such Treg cells are guaranteed to possess the favorable stability of the tTreg cell lineage (73). In addition, the localization and function of mature Treg cells seems strongly dependent on the Ags recognized by their TCRs (74, 75). Mature Treg cells in the thymus may thus be specific for local thymic Ags, possibly making them less able, for instance, to suppress graft-versus-host disease, which requires specificity for Ags in the intestinal mucosa or the skin. These considerations are all the more relevant, as the proportion of mature recirculating/resident eTreg cells in the thymus appears to be rather large and studies in mice have shown that the proportion of these cells increases with age (64).

Based on analysis of the other two clusters in combination with FACS, we deduced a sequence of tTreg cell differentiation, which we outline in a model (Fig. 8). We propose to refer to the subsequent stages of development as pre-Treg I (Cluster 1), and pre-Treg II (Cluster 2). The pre-Treg I stage is marked by the acquisition of CD25 expression and exhibits a $FOXO1^-CCR7^-$ phenotype. Some of these cells express *NR4A1*, presumably as a consequence of agonist selection. In addition, a fraction of pre-Treg I cells still expresses the lineage-inappropriate genes *CD40LG* and *CD8A*, as well as high amounts of *SATB1* and *ITM2A*. Of these, the chromatin organizer SATB1 helps establish a series of super enhancers in Treg-specific genes, possibly before initiation of Treg cell differentiation. Indeed, SATB1 is already expressed in murine $CD4^+CD8^+$ thymocytes (76). Its expression must be suppressed for proper Treg cell differentiation, and this occurs through direct FOXP3-mediated repression of the *SATB1* gene as well as indirectly via FOXP3-induced microRNAs that bind to the 3′ UTR of the SATB1 mRNA (76).

We identify the sharp induction of the transcription factor FOXO1 as a hallmark event that signals the transition of pre-Treg I cells to the ($FOXO1^+CCR7^+$) pre-Treg II stage. The discrete appearance of FOXO1 suggests that a specific (set of) signal(s) may induce its expression. The nature of such signals is currently not clear. Early during this (proposed early pre-Treg II) stage, expression of FOXO1 is followed by further upregulation of CD25 and (presumably) by elevated expression of *FOXP3,* consistent with the documented role of FOXO1 in transactivation of the *FOXP3* gene (50). Cells in this stage acquire high expression of CCR7 and KLF2, which are also encoded by target genes of FOXO1 (50, 77, 78), and which prepare the cells for migration from the thymus toward secondary lymphoid tissue in the periphery. Eventually, late pre-Treg II cells seem to obtain expression of CD31 and GPA33 before they acquire CD45RA, which marks them as mature naive Treg cells ready to exit from the thymus.

This model differs from the one presented by Park et al. (33). Similar to us, that study identified three major thymic populations of Treg lineage cells through single-cell transcriptomics. There, it was proposed that two of these populations, dubbed “T(agonist)” and

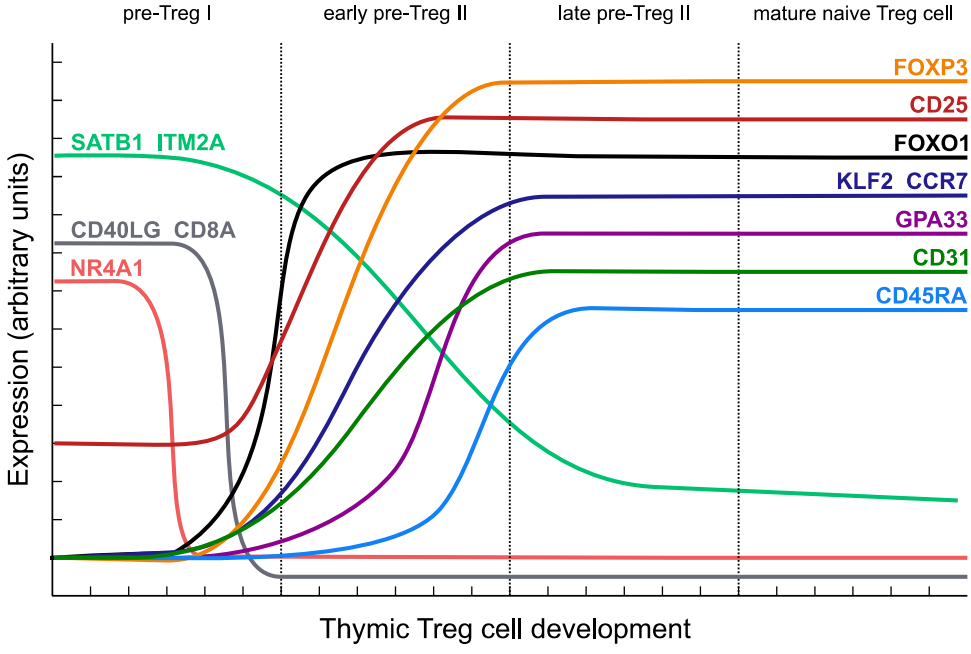

FIGURE 8. Proposed model of tTreg cell development. Schematic overview of our proposed model of tTreg cell development distinguishing a pre-Treg I, early pre-Treg II and late pre-Treg II stage based on gene and protein expression patterns identified using scRNAseq and flow cytometry. Note that the vertical expression is for visualization purposes and does not represent true expression values.

"Treg(diff)", might represent parallel routes of early Treg cell differentiation described in mice (31), initiating Treg cell differentiation by induction of CD25 or FOXP3, respectively. As for practical reasons our single-cell transcriptome analysis did not include $FOXP3^+CD25^-$cells, it was conceivable that we would have missed one of these developmental routes. Close comparison, however, showed that the populations found by Park et al. are very similar to ours. Thus, T(agonist) and Cluster 1 exhibit preferential expression of *CD40LG*, *CD8A*, *NR4A1*, *ITM2A*, and *SATB1*, whereas Treg(diff) and Cluster 2, exhibit higher expression of *FOXP3*, *CTLA4*, *BATF*, *KLF2*, *CCR7*, *FOXO1*, and *GPA33* (Supplemental Fig. 2H). Park et al. suggested that the T(agonist) and Treg(diff) populations might represent distinct developmental routes, because they were enriched for transcriptional signatures of the $FOXP3^+CD25^-$ and $CD25^+FOXP3^-$ populations (33), respectively. We found that the signature genes highlighted in the Park study exhibited the precise same relative expression patterns between T(agonist) and Treg(diff) as between our Cluster 1 and 2 (Supplemental Fig. 4C). The major difference therefore seems to lie in the interpretation of the results. Especially the high relative expression of lineage-inappropriate genes (*CD40L*, *CD8*), signature genes of $CD4^+CD8^+$ thymocytes (*SATB1*, *ITM2A*) and of *NR4A1* (a known TCR-responsive gene) in Cluster 1/T(agonist), but not in Cluster 2/Treg(diff), suggest to us that the former is a more immature population. We did confirm the existence of $FOXP3^+CD25^-$ cells in human thymus by flow cytometry. Based on the stage-specific markers identified in this study, these cells apparently exhibit an immature phenotype and appear to transition from a pre-Treg I to a pre-Treg II stage (Supplemental Fig. 4A, 4B).

The existence of these two distinct developmental routes raises the possibility that tTreg cell development might not always follow a fixed, linear path. Instead, the induction or upregulation of certain transcripts might occur in a slightly different order, perhaps dependent on the signals that the cells receive at that point or stochastic factors. It is an intriguing option that such differences in maturational progression contribute to the generation of heterogeneity in the mature Treg cell lineage (31, 38, 79). Nonetheless, most cells seem to follow a major differentiation path with discrete steps, as suggested by our data. Identifying the key signals for tTreg cell development would bring us closer to de novo generation of genuine tTreg cells in vitro from precursor cells or induced pluripotent stem cells, which might enable tailoring of Treg cells for ACT to treat inflammatory and (auto)immune conditions.

Acknowledgments

We thank Mark Hazekamp and the rest of the cardiothoracic surgical staff at the Leiden University Medical Center for providing human thymus material. We would also like to express our gratitude to all patients and parents involved in this work. We kindly thank Simon Tol, Erik Mul, and Mark Hoogeboezem for help with the FACS.

Disclosures

A patent was filed by D.A. on the use of GPA33 to isolate stable Treg cells. The other authors have no financial conflicts of interest.

References

1. Sakaguchi, S. 2005. Naturally arising Foxp3-expressing CD25+CD4+ regulatory T cells in immunological tolerance to self and non-self. *Nat. Immunol.* 6: 345–352.
2. Esensten, J. H., Y. D. Muller, J. A. Bluestone, and Q. Tang. 2018. Regulatory T-cell therapy for autoimmune and autoinflammatory diseases: The next frontier. *J. Allergy Clin. Immunol.* 142: 1710–1718.
3. Trzonkowski, P., R. Bacchetta, M. Battaglia, D. Berglund, H. R. Bohnenkamp, A. ten Brinke, A. Bushell, N. Cools, E. K. Geissler, S. Gregori, et al. 2015. Hurdles in therapy with regulatory T cells. *Sci. Transl. Med.* 7: 304ps18.
4. Mason, G. M., K. Lowe, R. Melchiotti, R. Ellis, E. de Rinaldis, M. Peakman, S. Heck, G. Lombardi, and T. I. M. Tree. 2015. Phenotypic complexity of the human regulatory T cell compartment revealed by mass cytometry. *J. Immunol.* 195: 2030–2037.
5. Zheng, Y., A. Chaudhry, A. Kas, P. deRoos, J. M. Kim, T.-T. Chu, L. Corcoran, P. Treuting, U. Klein, and A. Y. Rudensky. 2009. Regulatory T-cell suppressor program co-opts transcription factor IRF4 to control T(H)2 responses. *Nature* 458: 351–356.
6. Koch, M. A., G. Tucker-Heard, N. R. Perdue, J. R. Killebrew, K. B. Urdahl, and D. J. Campbell. 2009. The transcription factor T-bet controls regulatory T cell homeostasis and function during type 1 inflammation. *Nat. Immunol.* 10: 595–602.
7. Miragaia, R. J., T. Gomes, A. Chomka, L. Jardine, A. Riedel, A. N. Hegazy, N. Whibley, A. Tucci, X. Chen, I. Lindeman, et al. 2019. Single-cell transcriptomics of regulatory T cells reveals trajectories of tissue adaptation. *Immunity* 50: 493–504.e7.
8. Weiss, J. M., A. M. Bilate, M. Gobert, Y. Ding, M. A. Curotto de Lafaille, C. N. Parkhurst, H. Xiong, J. Dolpady, A. B. Frey, M. G. Ruocco, et al. 2012. Neuropilin 1 is expressed on thymus-derived natural regulatory T cells, but not mucosa-generated induced Foxp3+ T reg cells. *J. Exp. Med.* 209: 1723–1742, S1.
9. Thornton, A. M., P. E. Korty, D. Q. Tran, E. A. Wohlfert, P. E. Murray, Y. Belkaid, and E. M. Shevach. 2010. Expression of Helios, an Ikaros transcription factor family member, differentiates thymic-derived from peripherally induced Foxp3+ T regulatory cells. *J. Immunol.* 184: 3433–3441.
10. Toker, A., D. Engelbert, G. Garg, J. K. Polansky, S. Floess, T. Miyao, U. Baron, S. Düber, R. Geffers, P. Giehr, et al. 2013. Active demethylation of the Foxp3 locus leads to the generation of stable regulatory T cells within the thymus. *J. Immunol.* 190: 3180–3188.
11. Kanamori, M., H. Nakatsukasa, M. Okada, Q. Lu, and A. Yoshimura. 2016. Induced regulatory T cells: their development, stability, and applications. *Trends Immunol.* 37: 803–811.
12. Koenecke, C., N. Czeloth, A. Bubke, S. Schmitz, A. Kissenpfennig, B. Malissen, J. Huehn, A. Ganser, R. Förster, and I. Prinz. 2009. Alloantigen-specific de novo-induced Foxp3+ Treg revert in vivo and do not protect from experimental GVHD. *Eur. J. Immunol.* 39: 3091–3096.
13. Milpied, P., A. Renand, J. Bruneau, D. A. Mendes-da-Cruz, S. Jacquelin, V. Asnafi, M. T. Rubio, E. MacIntyre, Y. Lepelletier, and O. Hermine. 2009. Neuropilin-1 is not a marker of human Foxp3+ Treg. *Eur. J. Immunol.* 39: 1466–1471.
14. Thornton, A. M., J. Lu, P. E. Korty, Y. C. Kim, C. Martens, P. D. Sun, and E. M. Shevach. 2019. $Helios^+$ and $Helios^-$ Treg subpopulations are phenotypically and functionally distinct and express dissimilar TCR repertoires. *Eur. J. Immunol.* 49: 398–412.
15. Akimova, T., U. H. Beier, L. Wang, M. H. Levine, and W. W. Hancock. 2011. Helios expression is a marker of T cell activation and proliferation. *PLoS One* 6: e24226.
16. Dijke, I. E., R. E. Hoeppli, T. Ellis, J. Pearcey, Q. Huang, A. N. McMurchy, K. Boer, A. M. A. Peeters, G. Aubert, I. Larsen, et al. 2016. Discarded human thymus is a novel source of stable and long-lived therapeutic regulatory T cells. *Am. J. Transplant.* 16: 58–71.
17. Lio, C.-W. J., and C.-S. Hsieh. 2008. A two-step process for thymic regulatory T cell development. *Immunity* 28: 100–111.
18. Lee, H. M., and C.-S. Hsieh. 2009. Rare development of Foxp3+ thymocytes in the CD4+CD8+ subset. *J. Immunol.* 183: 2261–2266.
19. Nunes-Cabaço, H., I. Caramalho, N. Sepúlveda, and A. E. Sousa. 2011. Differentiation of human thymic regulatory T cells at the double positive stage. *Eur. J. Immunol.* 41: 3604–3614.
20. Darrasse-Jèze, G., G. Marodon, B. L. Salomon, M. Catala, and D. Klatzmann. 2005. Ontogeny of CD4+CD25+ regulatory/suppressor T cells in human fetuses. *Blood* 105: 4715–4721.
21. Owen, D. L., L. E. Sjaastad, and M. A. Farrar. 2019. Regulatory T cell development in the thymus. *J. Immunol.* 203: 2031–2041.
22. Mahmud, S. A., L. S. Manlove, H. M. Schmitz, Y. Xing, Y. Wang, D. L. Owen, J. M. Schenkel, J. S. Boomer, J. M. Green, H. Yagita, et al. 2014. Costimulation via the tumor-necrosis factor receptor superfamily couples TCR signal strength to the thymic differentiation of regulatory T cells. *Nat. Immunol.* 15: 473–481.
23. Coquet, J. M., J. C. Ribot, N. Bąbała, S. Middendorp, G. van der Horst, Y. Xiao, J. F. Neves, D. Fonseca-Pereira, H. Jacobs, D. J. Pennington, et al. 2013. Epithelial and dendritic cells in the thymic medulla promote CD4+Foxp3+ regulatory T cell development via the CD27-CD70 pathway. *J. Exp. Med.* 210: 715–728.
24. Burchill, M. A., J. Yang, K. B. Vang, J. J. Moon, H. H. Chu, C.-W. J. Lio, A. L. Vegoe, C.-S. Hsieh, M. K. Jenkins, and M. A. Farrar. 2008. Linked T cell receptor and cytokine signaling govern the development of the regulatory T cell repertoire. *Immunity* 28: 112–121.
25. Chorro, L., M. Suzuki, S. S. Chin, T. M. Williams, E. L. Snapp, L. Odagiu, N. Labrecque, and G. Lauvau. 2018. Interleukin 2 modulates thymic-derived regulatory T cell epigenetic landscape. *Nat. Commun.* 9: 5368.
26. Muraro, M. J., G. Dharmadhikari, D. Grün, N. Groen, T. Dielen, E. Jansen, L. van Gurp, M. A. Engelse, F. Carlotti, E. J. P. de Koning, and A. van Oudenaarden. 2016. A single-cell transcriptome atlas of the human pancreas. *Cell Syst.* 3: 385–394.e3.
27. Satija, R., J. A. Farrell, D. Gennert, A. F. Schier, and A. Regev. 2015. Spatial reconstruction of single-cell gene expression data. *Nat. Biotechnol.* 33: 495–502.

28. Ilicic, T., J. K. Kim, A. A. Kolodziejczyk, F. O. Bagger, D. J. McCarthy, J. C. Marioni, and S. A. Teichmann. 2016. Classification of low quality cells from single-cell RNA-seq data. *Genome Biol.* 17: 29.
29. Street, K., D. Risso, R. B. Fletcher, D. Das, J. Ngai, N. Yosef, E. Purdom, and S. Dudoit. 2018. Slingshot: cell lineage and pseudotime inference for single-cell transcriptomics. *BMC Genomics* 19: 477.
30. Tuulasvaara, A., R. Vanhanen, H.-M. Baldauf, J. Puntila, and T. P. Arstila. 2016. Interleukin-7 promotes human regulatory T cell development at the CD4+CD8+ double-positive thymocyte stage. *J. Leukoc. Biol.* 100: 491–498.
31. Owen, D. L., S. A. Mahmud, L. E. Sjaastad, J. B. Williams, J. A. Spanier, D. R. Simeonov, R. Ruscher, W. Huang, I. Proekt, C. N. Miller, et al. 2019. Thymic regulatory T cells arise via two distinct developmental programs. *Nat. Immunol.* 20: 195–205.
32. Tuovinen, H., E. Kekäläinen, L. H. Rossi, J. Puntila, and T. P. Arstila. 2008. Cutting edge: human CD4-CD8- thymocytes express FOXP3 in the absence of a TCR. *J. Immunol.* 180: 3651–3654.
33. Park, J.-E., R. A. Botting, C. Domínguez Conde, D.-M. Popescu, M. Lavaert, D. J. Kunz, I. Goh, E. Stephenson, R. Ragazzini, E. Tuck, et al. 2020. A cell atlas of human thymic development defines T cell repertoire formation. *Science* 367: eaay3224.
34. Haines, C. J., T. D. Giffon, L.-S. Lu, X. Lu, M. Tessier-Lavigne, D. T. Ross, and D. B. Lewis. 2009. Human CD4+ T cell recent thymic emigrants are identified by protein tyrosine kinase 7 and have reduced immune function. *J. Exp. Med.* 206: 275–285.
35. Zhang, N., B. Schröppel, G. Lal, C. Jakubzick, X. Mao, D. Chen, N. Yin, R. Jessberger, J. C. Ochando, Y. Ding, and J. S. Bromberg. 2009. Regulatory T cells sequentially migrate from inflamed tissues to draining lymph nodes to suppress the alloimmune response. *Immunity* 30: 458–469.
36. Huehn, J., K. Siegmund, J. C. U. Lehmann, C. Siewert, U. Haubold, M. Feuerer, G. F. Debes, J. Lauber, O. Frey, G. K. Przybylski, et al. 2004. Developmental stage, phenotype, and migration distinguish naive- and effector/memory-like CD4+ regulatory T cells. *J. Exp. Med.* 199: 303–313.
37. Sallusto, F., D. Lenig, R. Förster, M. Lipp, and A. Lanzavecchia. 1999. Two subsets of memory T lymphocytes with distinct homing potentials and effector functions. *Nature* 401: 708–712.
38. Ito, T., S. Hanabuchi, Y.-H. Wang, W. R. Park, K. Arima, L. Bover, F. X.-F. Qin, M. Gilliet, and Y.-J. Liu. 2008. Two functional subsets of FOXP3+ regulatory T cells in human thymus and periphery. *Immunity* 28: 870–880.
39. Thiault, N., J. Darrigues, V. Adoue, M. Gros, B. Binet, C. Perals, B. Leobon, N. Fazilleau, O. P. Joffre, E. A. Robey, et al. 2015. Peripheral regulatory T lymphocytes recirculating to the thymus suppress the development of their precursors. *Nat. Immunol.* 16: 628–634.
40. Nikolouli, E., Y. Elfaki, S. Herppich, C. Schelmbauer, M. Delacher, C. Falk, I. A. Mufazalov, A. Waisman, M. Feuerer, and J. Huehn. 2021. Recirculating IL-1R2^{+} Tregs fine-tune intrathymic Treg development under inflammatory conditions. *Cell. Mol. Immunol.* 18: 182–193.
41. Epeldegui, M., B. Blom, and C. H. Uittenbogaart. 2015. BST2/Tetherin is constitutively expressed on human thymocytes with the phenotype and function of Treg cells. *Eur. J. Immunol.* 45: 728–737.
42. Calnan, B. J., S. Szychowski, F. K. Chan, D. Cado, and A. Winoto. 1995. A role for the orphan steroid receptor Nur77 in apoptosis accompanying antigen-induced negative selection. *Immunity* 3: 273–282.
43. Fassett, M. S., W. Jiang, A. M. D'Alise, D. Mathis, and C. Benoist. 2012. Nuclear receptor Nr4a1 modulates both regulatory T-cell (Treg) differentiation and clonal deletion. *Proc. Natl. Acad. Sci. USA* 109: 3891–3896.
44. Moran, A. E., K. L. Holzapfel, Y. Xing, N. R. Cunningham, J. S. Maltzman, J. Punt, and K. A. Hogquist. 2011. T cell receptor signal strength in Treg and iNKT cell development demonstrated by a novel fluorescent reporter mouse. *J. Exp. Med.* 208: 1279–1289.
45. Kirchner, J., and M. J. Bevan. 1999. ITM2A is induced during thymocyte selection and T cell activation and causes downregulation of CD8 when overexpressed in CD4(+)CD8(+) double positive thymocytes. *J. Exp. Med.* 190: 217–228.
46. Kitagawa, Y., N. Ohkura, Y. Kidani, A. Vandenbon, K. Hirota, R. Kawakami, K. Yasuda, D. Motooka, S. Nakamura, M. Kondo, et al. 2017. Guidance of regulatory T cell development by Satb1-dependent super-enhancer establishment. [Published errata appear in 2017 *Nat. Immunol.* 18: 474 and *2017 Nat. Immunol.* 18: 1270.] *Nat. Immunol.* 18: 173–183.
47. Carlson, C. M., B. T. Endrizzi, J. Wu, X. Ding, M. A. Weinreich, E. R. Walsh, M. A. Wani, J. B. Lingrel, K. A. Hogquist, and S. C. Jameson. 2006. Kruppel-like factor 2 regulates thymocyte and T-cell migration. *Nature* 442: 299–302.
48. Bai, A., H. Hu, M. Yeung, and J. Chen. 2007. Kruppel-like factor 2 controls T cell trafficking by activating L-selectin (CD62L) and sphingosine-1-phosphate receptor 1 transcription. *J. Immunol.* 178: 7632–7639.
49. Kerdiles, Y. M., E. L. Stone, D. R. Beisner, M. A. McGargill, I. L. Ch'en, C. Stockmann, C. D. Katayama, and S. M. Hedrick. 2010. Foxo transcription factors control regulatory T cell development and function. [Published erratum appears in 2011 *Immunity* 34: 135.] *Immunity* 33: 890–904.
50. Ouyang, W., O. Beckett, Q. Ma, J. H. Paik, R. A. DePinho, and M. O. Li. 2010. Foxo proteins cooperatively control the differentiation of Foxp3+ regulatory T cells. *Nat. Immunol.* 11: 618–627.
51. Belkina, A. C., C. O. Ciccolella, R. Anno, R. Halpert, J. Spidlen, and J. E. Snyder-Cappione. 2019. Automated optimized parameters for T-distributed stochastic neighbor embedding improve visualization and analysis of large datasets. *Nat. Commun.* 10: 5415.
52. Cupedo, T., M. Nagasawa, K. Weijer, B. Blom, and H. Spits. 2005. Development and activation of regulatory T cells in the human fetus. *Eur. J. Immunol.* 35: 383–390.
53. Opstelten, R., S. de Kivit, M. C. Slot, M. van den Biggelaar, D. Iwaszkiewicz-Grześ, M. Gliwiński, A. M. Scott, B. Blom, P. Trzonkowski, J. Borst, et al. 2020. GPA33: a marker to identify stable human regulatory T cells. *J. Immunol.* 204: 3139–3148.
54. Kurtulus, S., K. Sakuishi, S.-F. Ngiow, N. Joller, D. J. Tan, M. W. L. Teng, M. J. Smyth, V. K. Kuchroo, and A. C. Anderson. 2015. TIGIT predominantly regulates the immune response via regulatory T cells. *J. Clin. Invest.* 125: 4053–4062.
55. Fuhrman, C. A., W. I. Yeh, H. R. Seay, P. Saikumar Lakshmi, G. Chopra, L. Zhang, D. J. Perry, S. A. McClymont, M. Yadav, M.-C. Lopez, et al. 2015. Divergent phenotypes of human regulatory T cells expressing the receptors TIGIT and CD226. *J. Immunol.* 195: 145–155.
56. Joller, N., E. Lozano, P. R. Burkett, B. Patel, S. Xiao, C. Zhu, J. Xia, T. G. Tan, E. Sefik, V. Yajnik, et al. 2014. Treg cells expressing the coinhibitory molecule TIGIT selectively inhibit proinflammatory Th1 and Th17 cell responses. *Immunity* 40: 569–581.
57. Douaisi, M., R. S. Resop, M. Nagasawa, J. Craft, B. D. Jamieson, B. Blom, and C. H. Uittenbogaart. 2017. CD31, a valuable marker to identify early and late stages of T cell differentiation in the human thymus. *J. Immunol.* 198: 2310–2319.
58. Ueno, T., F. Saito, D. H. D. Gray, S. Kuse, K. Hieshima, H. Nakano, T. Kakiuchi, M. Lipp, R. L. Boyd, and Y. Takahama. 2004. CCR7 signals are essential for cortex-medulla migration of developing thymocytes. *J. Exp. Med.* 200: 493–505.
59. Kwan, J., and N. Killeen. 2004. CCR7 directs the migration of thymocytes into the thymic medulla. *J. Immunol.* 172: 3999–4007.
60. Ueno, T., K. Hara, M. S. Willis, M. A. Malin, U. E. Höpken, D. H. D. Gray, K. Matsushima, M. Lipp, T. A. Springer, R. L. Boyd, et al. 2002. Role for CCR7 ligands in the emigration of newly generated T lymphocytes from the neonatal thymus. *Immunity* 16: 205–218.
61. Miyara, M., Y. Yoshioka, A. Kitoh, T. Shima, K. Wing, A. Niwa, C. Parizot, C. Taflin, T. Heike, D. Valeyre, et al. 2009. Functional delineation and differentiation dynamics of human CD4+ T cells expressing the FoxP3 transcription factor. *Immunity* 30: 899–911.
62. Cuadrado, E., M. van den Biggelaar, S. de Kivit, Y.-Y. Chen, M. Slot, I. Doubal, A. Meijer, R. A. W. van Lier, J. Borst, and D. Amsen. 2018. Proteomic analyses of human regulatory T cells reveal adaptations in signaling pathways that protect cellular identity. *Immunity* 48: 1046–1059.e6.
63. Cowan, J. E., S. Baik, N. I. McCarthy, S. M. Parnell, A. J. White, W. E. Jenkinson, and G. Anderson. 2018. Aire controls the recirculation of murine Foxp3^{+} regulatory T-cells back to the thymus. *Eur. J. Immunol.* 48: 844–854.
64. Yang, E., T. Zou, T. M. Leichner, S. L. Zhang, and T. Kambayashi. 2014. Both retention and recirculation contribute to long-lived regulatory T-cell accumulation in the thymus. *Eur. J. Immunol.* 44: 2712–2720.
65. Zhan, Y., D. Bourges, J. A. Dromey, L. C. Harrison, and A. M. Lew. 2007. The origin of thymic CD4+CD25+ regulatory T cells and their co-stimulatory requirements are determined after elimination of recirculating peripheral CD4+ cells. *Int. Immunol.* 19: 455–463.
66. Burzyn, D., C. Benoist, and D. Mathis. 2013. Regulatory T cells in nonlymphoid tissues. *Nat. Immunol.* 14: 1007–1013.
67. Wohlfert, E. A., J. R. Grainger, N. Bouladoux, J. E. Konkel, G. Oldenhove, C. H. Ribeiro, J. A. Hall, R. Yagi, S. Naik, R. Bhairavabhotla, et al. 2011. GATA3 controls Foxp3+ regulatory T cell fate during inflammation in mice. 121: 4503–4515.
68. Feuerer, M., L. Herrero, D. Cipolletta, A. Naaz, J. Wong, A. Nayer, J. Lee, A. B. Goldfine, C. Benoist, S. Shoelson, and D. Mathis. 2009. Lean, but not obese, fat is enriched for a unique population of regulatory T cells that affect metabolic parameters. *Nat. Med.* 15: 930–939.
69. Burzyn, D., W. Kuswanto, D. Kolodin, J. L. Shadrach, M. Cerletti, Y. Jang, E. Sefik, T. G. Tan, A. J. Wagers, C. Benoist, and D. Mathis. 2013. A special population of regulatory T cells potentiates muscle repair. *Cell* 155: 1282–1295.
70. Vasanthakumar, A., K. Moro, A. Xin, Y. Liao, R. Gloury, S. Kawamoto, S. Fagarasan, L. A. Mielke, S. Afshar-Sterle, S. L. Masters, et al. 2015. The transcriptional regulators IRF4, BATF and IL-33 orchestrate development and maintenance of adipose tissue-resident regulatory T cells. [Published erratum appears in 2015 *Nat. Immunol.* 16: 544.] *Nat. Immunol.* 16: 276–285.
71. Neumann, C., J. Blume, U. Roy, P. P. Teh, A. Vasanthakumar, A. Beller, Y. Liao, F. Heinrich, T. L. Arenzana, J. A. Hackney, et al. 2019. c-Maf-dependent T_{reg} cell control of intestinal T_H17 cells and IgA establishes host-microbiota homeostasis. *Nat. Immunol.* 20: 471–481.
72. Cretney, E., A. Xin, W. Shi, M. Minnich, F. Masson, M. Miasari, G. T. Belz, G. K. Smyth, M. Busslinger, S. L. Nutt, and A. Kallies. 2011. The transcription factors Blimp-1 and IRF4 jointly control the differentiation and function of effector regulatory T cells. *Nat. Immunol.* 12: 304–311.
73. Baron, U., S. Floess, G. Wieczorek, K. Baumann, A. Grützkau, J. Dong, A. Thiel, T. J. Boeld, P. Hoffmann, M. Edinger, et al. 2007. DNA demethylation in the human FOXP3 locus discriminates regulatory T cells from activated FOXP3(+) conventional T cells. *Eur. J. Immunol.* 37: 2378–2389.
74. Schmidt, A. M., W. Lu, V. J. Sindhava, Y. Huang, J. K. Burkhardt, E. Yang, M. J. Riese, J. S. Maltzman, M. S. Jordan, and T. Kambayashi. 2015. Regulatory T cells require TCR signaling for their suppressive function. *J. Immunol.* 194: 4362–4370.
75. Levine, A. G., A. Arvey, W. Jin, and A. Y. Rudensky. 2014. Continuous requirement for the TCR in regulatory T cell function. *Nat. Immunol.* 15: 1070–1078.

76. Beyer, M., Y. Thabet, R. U. Müller, T. Sadlon, S. Classen, K. Lahl, S. Basu, X. Zhou, S. L. Bailey-Bucktrout, W. Krebs, et al. 2011. Repression of the genome organizer SATB1 in regulatory T cells is required for suppressive function and inhibition of effector differentiation. *Nat. Immunol.* 12: 898–907.
77. Ouyang, W., W. Liao, C. T. Luo, N. Yin, M. Huse, M. V. Kim, M. Peng, P. Chan, Q. Ma, Y. Mo, et al. 2012. Novel Foxo1-dependent transcriptional programs control T(reg) cell function. *Nature* 491: 554–559.
78. Kerdiles, Y. M., D. R. Beisner, R. Tinoco, A. S. Dejean, D. H. Castrillon, R. A. DePinho, and S. M. Hedrick. 2009. Foxo1 links homing and survival of naive T cells by regulating L-selectin, CCR7 and interleukin 7 receptor. *Nat. Immunol.* 10: 176–184.
79. Wyss, L., B. D. Stadinski, C. G. King, S. Schallenberg, N. I. McCarthy, J. Y. Lee, K. Kretschmer, L. M. Terracciano, G. Anderson, C. D. Surh, et al. 2016. Affinity for self antigen selects Treg cells with distinct functional properties. *Nat. Immunol.* 17: 1093–1101.